# Non-Linear Effects in Multicomponent Supramolecular Hydrogels

*Emily R. Draper,[a] Matthew Wallace,[b] Ralf Schweins,[c] Robert J. Poole[d] and Dave J. Adams[a,]**

a School of Chemistry, Joseph Black Building, University of Glasgow, Glasgow G12 8QQ, U.K.

b Department of Chemistry, University of Liverpool, Crown Street, Liverpool, L69 7ZD, U.K.

c Institut Laue-Langevin, Large Scale Structures Group, 71 Avenue des Martyrs, CS 20156, F-38042 Grenoble CEDEX 9, France

d School of Engineering, University of Liverpool, Brownlow Street, L69 3GH, U.K.

ABSTRACT Multicomponent low molecular weight gels are useful for a range of applications. However, when mixing two components, both of which can independently form a gel, there are many potential scenarios. There is a limited understanding as to how to control and direct the assembly. Here, we focus on a pH-triggered two component system. At high pH, colloidal structures are formed and there is a degree of mixing of the two gelators. As the pH is decreased, there is a complex situation, where one gelator directs the assembly in a “sergeants and soldiers” manner. The second gelator is not fully incorporated and the remainder forms an independent network. The result is that there is a non-linear dependence on the final mechanical properties of

the gels, with the storage or loss modulus being very dependent on the absolute ratio of the two components in the system.

## Introduction

Low molecular weight gels have been used for a wide range of applications, including directing cell growth, optoelectronics, and controlled release.[1-5] Most commonly, a single low molecular weight gelator (LMWG) is used to form the network. However, there is increasing interest in using multicomponent networks.[6-21] Multicomponent self-assembled gels are a method of increasing the complexity, tuning the properties, and possibly information content into a network.[22-25] However, little is known about what properties are possible. For example, it is clear that mixing two gelators, both of which can independently lead to a gel network, can lead to either self-sorted or intimately mixed structures (Fig. 1).[6-7] The properties of the final gel will be controlled by the properties of the fibres that give rise to the network, as well as how the fibres entangle or crosslink and how the fibres are distributed in space. Linking the gel properties to network type is not well understood for even single component systems. There are very few reports where this is considered for multicomponent systems. Indeed, as one example, the observation that a multicomponent gel has higher a storage modulus than would be expected by simply comparing to the data for gels formed from the individual components has been used to assign gels as both self-sorted and intimately mixed.[26-27]

We have been investigating multicomponent hydrogels formed using pH-responsive LMWG (example structures are shown in Scheme 1).[27-31] Here, the LMWG form self-assembled aggregates at high pH above the apparent p$K_a$ of the terminal carboxylic acids; the structures can

be spherical or worm-like micelles.[32-34] This is unsurprising, as they are effectively surfactants at this elevated pH.[32, 35] As the pH is decreased, they start to assemble into fibrous structures at the apparent p$K_a$, which entangle and associate to form the gel network.[36] We typically lower the pH slowly and controllably using the hydrolysis of gluono-δ-lactone (GdL) to gluconic acid,[37] or the hydrolysis of an anhydride.[38] These methods have proven very effective at allowing us to achieve reproducible kinetics of pH change and gelation.

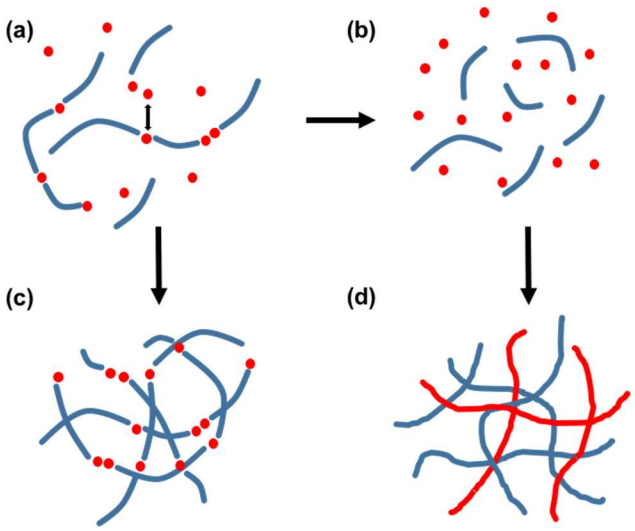


**Fig. 1** Cartoon showing the hypothetical assembly of two different LMWG. Either (or both) component may be assembled at high pH (shown here the blue LMWG forms worm-like micelles). The other component may be interacting or independent. On decreasing the pH, there may be no interactions between LMWG (shown in (b)), meaning two independent networks form (d). Alternatively, there may be interactions between LMWG, leading to a co-assembled network (c). The real situation could be somewhere between these two ideal cases.

In a mixed system, there are multiple different situations conceptually possible depending on the absolute pH of the system and the relative apparent p$K_a$ of the different LMWG (Fig. 1).

First, the self-assembled structures at high pH may not be affected by each other. Second, there may be mixing, and perhaps even new structures formed at high pH. Where the pH is decreased, assuming two independent p$K_a$ are maintained, the LMWG with the highest p$K_a$ will start to assemble into fibres first; in doing so, it will now be assembling in the presence of the second LMWG which will still have surfactant-like properties (we have previously shown that this type of LMWG can act as a surfactant[32, 35]). This may fundamentally change how the first LMWG assembles, either co-operatively or disruptively.[39] After the first LMWG has assembled, the second LMWG will begin to form fibres. Here, there is already a fibre network present from the first LMWG, so this may template the second LMWG, or may simply use up some of the possible space.

There is a further complication depending on the relative amounts of each LMWG in the system. It is most common to mix equal masses of each LWMG, but of course this does not have to be the case. The apparent p$K_a$ of each component can be concentration dependent,[40] as can the micellar species at high pH.[32] Hence, this variable opens another complication to the system.

In this paper, we investigate the effect of relative concentration in a mixture of two LMWG. We concentrate on determining whether co-assembly or self-sorting is occurring and on whether the structures formed at high pH are important in determining the gel network formed at low pH.

**Results and discussion**

In our previous work, we have found it very difficult to ascertain whether the solutions at high pH contain self-sorted or mixed micellar systems. To allow us to probe the system in a number of ways, here we have chosen two specific LMWG from our extended library. 2NapFF (Scheme 1) forms worm-like micelles at high pH,[32] whereas 2NapVG (Scheme 1) does not.[41] We

hypothesized that this would allow us to easily probe the effect of mixing at high pH, where on the basis of previous work the viscosity and small angle neutron scattering data are expected to be dominated by the 2NapFF.

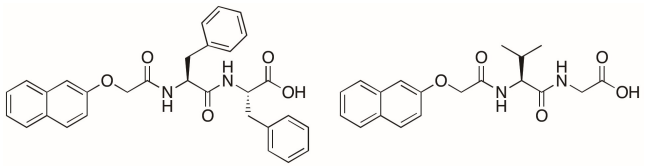

**Scheme 1.** Chemical structures of 2NapFF (left) and 2NapVG (right).

At a concentration of 10 mg/mL and a pH of between 10 and 12, 2NapFF forms a slightly turbid viscous solution.[32] 2NapVG forms a transparent non-viscous solution at this pH and concentration.[41] This pH range is significantly above the apparent p$K_a$ of both the 2NapFF and 2NapVG (6.0 and 5.0 respectively[40-41] at a concentration of 5 mg/mL). We mixed aliquots of these solutions to provide a series of solutions with a number of different ratios of 2NapFF to 2NapVG. Here, it is important that both solutions are at the same pH; additionally, we note that for all of the following the absolute pH value is very important, with differences in absolute viscosity being observed depending on the pH. Hence, for all of the data provided below for viscosities and rheological data, a single batch of each stock solution were used to generate the mixtures. The qualitative trends are the same for different pH between 10 and 12, but the absolute values differ.

Mixing solutions of 2NapFF and 2NapVG such that the total concentration of LMWG was always 10 mg/mL gave translucent solutions at pH 11.0 ± 0.2 (N.B., for some of the data below, $D_2O$ was used instead of $H_2O$; pH differs from pD and hence the samples in $D_2O$ were adjusted

such that the pH was the same for all samples[42-43]). As noted above, the pure 2NapFF solution was visibly viscous. The viscosity of the solution decreased approximately linearly as the solution was diluted with 2NapVG (Fig. 2a). This implies that the solutions are self-sorted, with the worm-like micelles present in the 2NapFF solution leading to the increased viscosity were simply being diluted on addition of the 2NapVG. A complication here is shear history. Samples that had been previously sheared and allowed to stand before further use showed significant increases in viscosity, and also exhibited a marked "stringiness" consistent with an increased extensional viscosity (see Fig. S1, Supporting Information). Hence, solutions for which the viscosity was measured became more viscous with time. A number of studies ruled out that this effect was due to time and the shear applied by the rheometer for the viscosity measurements (up to $10^2$ $s^{-1}$, as well as measurements at constant shear rate over extended periods of time). This increase in viscosity seems to arise from the very high shear rates applied when the samples are unloaded from the rheometer using a pipette (~$10^3$-$10^6$ $s^{-1}$). To quantify the effects of shear history on the extensional viscosity of the solutions, experiments where performed using a Capillary Break-up Extensional Rheometer ("CaBER")[44] supplied by Haake Thermo Scientific. The diameter of the filament (D) is observed as a function of time (t) using the equipment's laser micrometer (resolution ~10 microns). Although the filament diameter data can be post-processed into an (apparent) extensional viscosity, the standard method to quantify extensional effects[44-45] is via an exponential fit to the filament diameter as a function of time in the elasto-capillary regime to determine a characteristic relaxation time, $\lambda$, (more correctly a characteristic time for extensional stress growth). Representative plots are shown in Fig. 2c, where the effect of shear history can be seen to dramatically increase this characteristic time $\lambda$. Because of this interesting behavior, all of the following data was collected for fresh samples that had not been exposed to

any additional shear history beyond that needed to freshly prepare the samples. Additionally, the uncertainties calculated for the viscosity data shown in Fig. 2 were calculated from multiple fresh samples.

Solutions containing different ratios of 2NapFF and 2NapVG were then gelled. To do this, we used GdL, which hydrolyses slowly and reproducibly to gluconic acid.[37] For all ratios, we used a fixed amount of GdL (10 mg/mL). With this amount of GdL, all of the ratios formed self-supporting hydrogels overnight (Fig. 2b) with the pH of all the gels at this point being 3.7 ± 0.1. Interestingly, despite the near linear trend at high pH of a decreasing viscosity with increasing content of 2NapVG, the storage modulus (G′) for the final gels is very non-linear (Fig. 2a). Tanδ (G″/G′) was between 0.17 and 0.20 for all gels from 100% to 20% 2NapFF, rising to 0.24 at 10% 2NapFF and 0.31 for the 0% 2NapFF gel. Strain sweeps are shown in Fig. S2 and Fig. S3, Supporting Information.

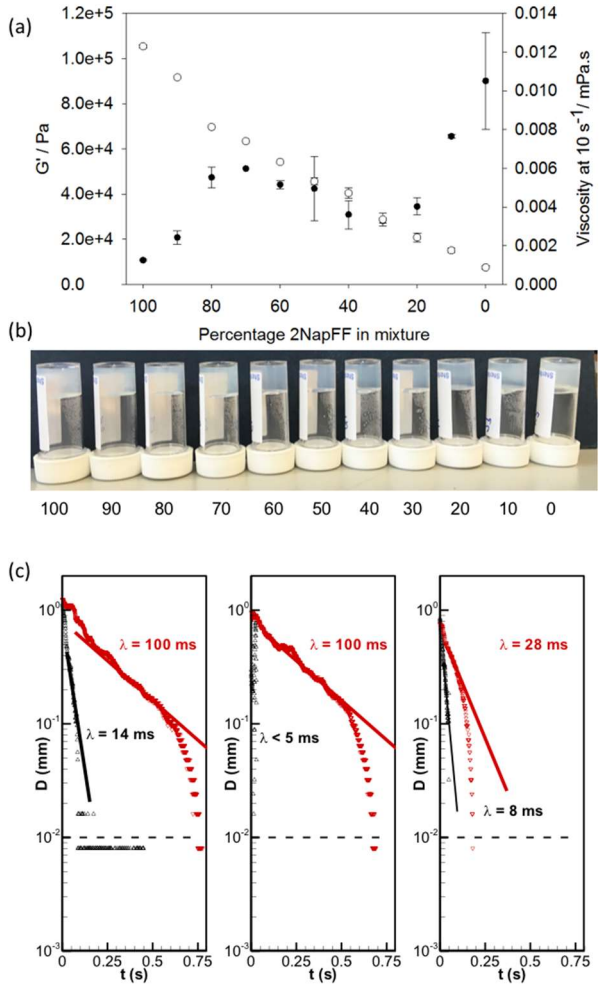


**Fig. 2** (a) Plot of viscosity of the solutions at high pH at different ratios of 2NapFF to 2NapVG (open symbols, right axis) and the storage modulus of the gels formed from these solutions at low pH (full symbols, left axis). (b) Photographs of the gels formed at the different ratios; the number under each vial represents the percentage of 2NapFF in the mixture. (c) Diameter-time data from CaBER experiments including exponential fits to obtain estimates of relaxation time λ; from left to right, data are shown for a sample at 100% 2NapFF, 70% 2NapFF and 30% 2NapFF. The black data are for fresh samples, with the fit shown as a black line. The red data are for samples that have been sheared through a pipette tip, with the red line being the fit to the data. The horizontal dashed line highlights the resolution of the laser micrometer.

The small angle neutron scattering (SANS) data for the gels can be best fit to a combination of a flexible elliptical cylinder, in combination with an absolute power law to fit the low Q region; the low Q region is sensitive to the fractal scattering from the network structure (Fig. S4 and S5, Supporting Information). Fits to the cylinder or flexible cylinder models were significantly less good than the elliptical model. To fit the data, the Kuhn length was fixed to a number of values and the fit was optimised based on the residuals. The best fit for the 100% 2NapFF gel was found with a radius of 3.55 ± 0.05 nm, an axis ratio of 2.58 ± 0.04, a Kuhn length of 20.50 ± 1.03 nm, and a length of 83.27 ± 4.24 nm. A power law of 2.58 ± 0.04 was also needed. On dilution of the 2NapFF with 2NapVG, the same model could be used successfully across the series of gels at low pH, with only minor changes in all parameters. This included the gel for the 2NapVG alone (i.e. 0 % 2NapFF), which was found to best fit to the same model, with a radius of 4.27 ± 0.11 nm, an axis ratio of 2.57 ± 0.21, a Kuhn length of 29.19 ± 7.34 nm, and a length of 159.43 ± 2.18 nm. A power-law exponent of 2.21 ± 0.03 was also needed. Hence, the SANS data implies that all networks are very similar. SEM images of the dried gels also show similar networks in all cases (Fig. S6, Supporting Information), and so we conclude that the differences in rheological data seen in Fig. 2 cannot be explained simply in terms of different types of fibres forming the networks.

To explain the non-linear rheology at low pH arising from solutions with approximately linear trends in viscosity, we examined the solutions at high pH in more detail. The increase in extensional viscosity on shearing even at very low concentrations of 2NapFF in the mixture (see above) implies that the 2NapVG is involved in the self-assembled structures, since it is difficult to imagine how such high viscosities can be achieved at the low concentrations of 2NapFF. To

probe this, we turned again to SANS. We have previously shown that the SANS data for solutions of 2NapFF at high pH can be fitted to a hollow cylinder model, again combined with a power law component to fit the low Q region.[32] The scattering data from all of the solutions of 2NapFF and 2NapVG at high pH were found to fit well to this model, apart from the data for pure 2NapVG (Fig. 3a and Fig. S7 and S8, Supporting Information). The pure 2NapVG exhibited very low scattering at high pH and the data could be fitted well to a power law alone. From the fits to the data from the other solutions, it can be seen that the internal and external radii of the hollow cylinder do not vary much across the dilution series. For pure 2NapFF, the core radius determined from the fit is 1.50 ± 0.11 nm, and the external radius is 4.06 ± 0.10 nm, in close agreement with our previous data.[32] At 70 %, 50%, and 30% 2NapFF, the core radii are 1.66 ± 0.18, 1.58 ± 0.22, and 1.57 ± 0.3 nm respectively, and the external radii 3.79 ± 0.13, 3.86 ± 0.15, and 3.90 ± 0.22 nm respectively. Further, from the scattering intensities, it is clear that there is not a linear decrease in intensity across the dilution series (Fig. 3d).

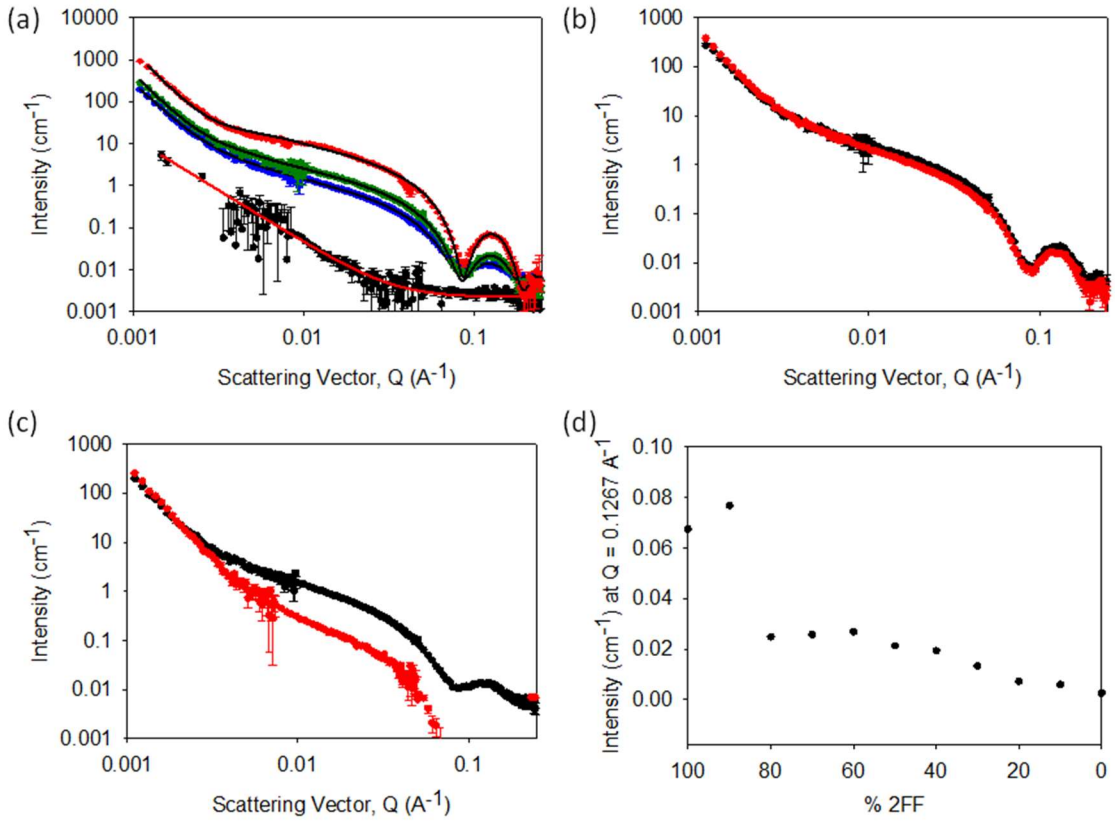


**Fig. 3** (a) SANS profiles for solutions at 100% 2NapFF (red), 70 % 2NapFF (green), 50% 2NapFF (blue), and 0% 2NapFF (black). The fits to a hollow cylinder model combined with a power law are shown as black lines and, for the 0% 2NapFF only, the fit to a power law alone is shown as a red line. (b) Top: Overlay of the SANS profiles for a solution of 2NapFF diluted 1:1 with 2NapVG (black data) or 1:1 with $D_2O$ (red data). Bottom: Overlay of the SANS profiles for a solution of 2NapFF diluted 3:7 with 2NapVG (black data) or 3:7 with $D_2O$ (red data). For all of these data, the solutions were prepared in $D_2O$, with a pD of 11.4 ± 0.2. (d) Plot of scattering intensity at Q = 0.1267 $Å^{-1}$ for solutions containing different ratios of 2NapFF and 2NapVG.

This again implies that the two LMWG are not completely self-sorted at high pH and potentially the structures formed are directed by the 2NapFF in a "sergeants and soldiers" manner.[46-47] Further evidence for this comes from a direct comparison between solutions of 2NapFF diluted with solutions of 2NapVG and those diluted with $D_2O$ (for SANS experiments, it is necessary to replace the $H_2O$ solvent with $D_2O$). Here, at high ratios of the 2NapFF, the scattering is very similar in intensity between the two methods of dilution (Fig. 3b). However, for the low ratios of 2NapFF, there are significant differences between the dilution methods (Fig. 3c). On diluting 2NapFF with $D_2O$, the scattering is significantly decreased, especially at high Q. This is similar to what we showed previously for diluted solutions of 2NapFF.[32] However, on dilution with the 2NapVG, the scattering was significantly higher as compared to the dilution with $D_2O$, and still showed the characteristic scattering of the hollow cylinders (Fig. 3c). All of these data strongly imply that the solutions are not self-sorted at high pH, but rather the assembly is directed by even relatively low amounts of the 2NapFF.

Finally, further evidence for interaction at high pH comes from NMR spectroscopy (Fig. 4). In the absence of 2NapFF, selective excitation of the methyl protons of the valine residue enhances the signal of the neighbouring CH protons (Fig. 4a). Such a positive NOE is indicative of fast molecular motions, indicating minimal aggregation of the gelators. As the proportion of 2NapFF is raised, the size of the enhancement diminishes and becomes slightly negative, indicating a significant decrease in the molecular mobility of the 2NapVG due to interaction with the 2NapFF.[48] Furthermore, the chemical shifts of the aromatic protons of 2NapVG are shifted upfield by the presence of the 2NapFF, consistent with an increased level of aggregation (Fig. 4b).[49]

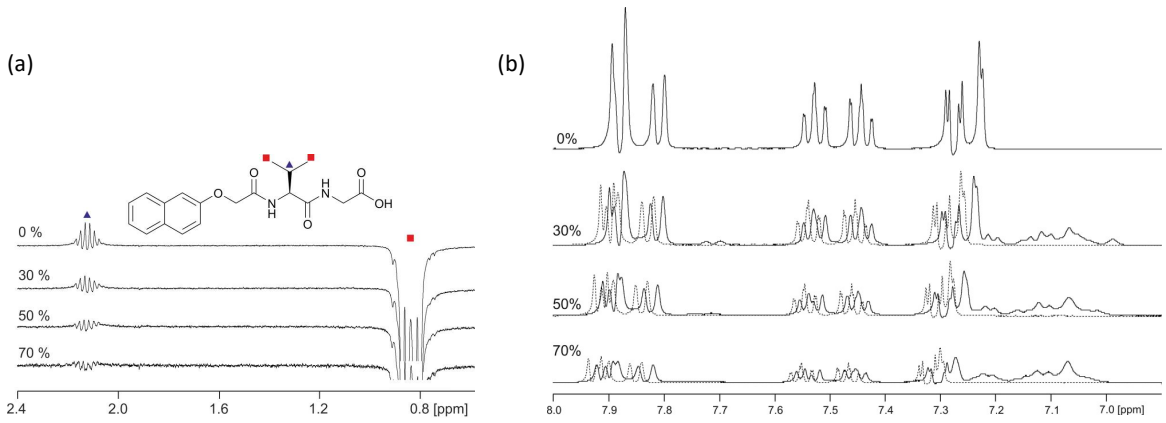


**Fig. 4.** (a) $^{1}$H NOE difference spectra of 2NapVG acquired at different percentages of 2NapFF. The methyl protons (square) were selectively excited and the NOE to the CH protons (triangle) monitored. The spectra have been scaled according to the amount of 2NapVG in the samples. (b) Partial $^{1}$H NMR spectra of 2NapVG at the proportion of 2NapFF indicated. The total concentration of LMWG was 10 mg/mL in all cases. Spectra recorded in the absence of 2NapFF, but at the same concentration of 2NapVG, are shown as dashed lines. A clear upfield shift of the aromatic protons of the 2NapVG is apparent when 2NapFF is included.

We interpret these data as there being a significant proportion of the 2NapVG that is exchanging in solution with the assembled structures of the 2NapFF. Since the 2NapVG is detectable by NMR (and indeed the concentration detected scales with the expected amount in the mixture (Fig. S9, Supporting Information), the 2NapVG must be exchanging with the assembled structure at a faster rate than the 2NapFF molecules. Hence, these data suggest that both molecules are present in the same aggregates at high pH. The aromatic $^{1}$H chemical shifts of the 2NapVG are moved upfield in the presence of 2NapFF (Fig. 4b). The shifts of the amino acid side chains are much less affected. Based on the work of Orfi *et al.*,[50] we therefore infer that the hydrophobic naphthalene group penetrates the structures formed by the 2NapFF while the

negatively charged peptide motif of the 2NapVG remains in contact with the external solution. The 2NapVG is thus behaving as a surfactant. However, on drying it is clear that exchange must be occurring, as the dried solutions show both worm-like micelles (expected from the 2NapFF) and ill-defined aggregates (expected from 2NapVG on the basis of other work). Example SEM images are shown in Fig. S10, Supporting Information.

Having determined that there is mixing at high pH, the next question arising is whether self-sorting occurs when the pH is decreased. It is conceptually possible that the aggregates at high pH might template assembly such that a mixed fibre system is formed. Alternatively, the two components could re-order such that self-sorted fibres are formed (Fig. 1). For previous mixtures of related LMWG, we have exploited the hydrolysis of GdL to gluconic acid to provide a controlled, reproducible slow change in pH to allow a combination of pH measurements, NMR integration, and rheological data to be collected over time to probe for self-sorting on gelation.[27, 30-31] Others have now also used this approach.[15, 51-52]

For the systems here, we have followed the gelation using $^{1}$H NMR spectroscopy. Here, we measure the sample over time; as the gelators assemble, the signals attenuate and the signal intensity decreases. Hence, it is possible to judge whether self-sorting has occurred from whether one gelator disappears from the NMR spectra at a different time to the second. In some cases, it is possible to observe two distinct plateaus in the pH data if the p$K_a$ of the two gelators is sufficiently different.[28, 30] In the current work, we have also exploited a method developed in house to measure the pH *in situ* in the NMR tube.[53]

Here, for the mixtures, a difficulty is that the signal intensity for the 2NapFF is low even at high pH, when less than 20% is detectable by NMR at 10 mg/mL concentration.[32] We have described this before;[32] we interpret this as the 2NapFF forming persistent worm-like micelles

that mean that the gelator is spending most of the time at high pH as part of a self-assembled structure. Strong saturation-transfer-difference (STD) effects are apparent to the NMR-visible 2NapFF as it interacts/exchanges with these structures (Fig. S11, Supporting Information). As such, it is not possible to monitor effectively the assembly of the 2NapFF by NMR. The 2NapVG, however, is detectable across the concentration series, which implies that at high pH the gelators are essentially unassembled (Fig. S9, Supporting Information). No significant STD effects are observed to the 2NapVG at high pH, indicating a minimal degree of aggregation compared to the 2NapFF.

For 2NapVG alone, the pH and NMR data are as expected (Fig. 5d). The pH drops to a plateau at the expected p$K_a$ of the gelator (5.0). The shape of the pH data is similar to that shown elsewhere for samples where the pH is changed using GdL;[36, 54] the pH drops to a value slightly below the apparent p$K_a$, before increasing to the p$K_a$ value, and then buffers before decreasing again. At this pH drop and increase, the signal intensity of the 2NapVG starts to drop, and completely attenuates over several hours. For 2NapFF alone, the pH falls to around the expected p$K_a$ of the compound and then exhibits a smooth decrease. There is no rise in the pH followed by a plateau as the structures are already assembled (Fig. S12, Supporting Information). No 2NapFF is detectable by NMR following the addition of GdL.

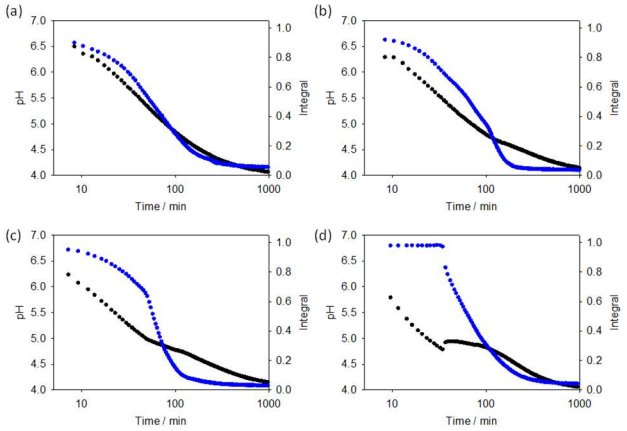


**Fig. 5.** Plots of change in pH (black data) and normalised intensity of the NMR integrals of the valine peaks of 2NapVG (blue data) with time after addition of GdL to solutions of (a) 70% 2NapFF; (b) 50% 2NapFF; (c) 30% 2NapFF; (d) 0% 2NapFF.

For the mixtures, the situation is more complicated than would be expected from our previous reports on self-sorted two component gelators.[27, 31] This in itself implies that the situation is more complicated than simple self-sorting. In the absence of 2NapFF, the assembly of 2NapVG occurs at a progressively lower pH as the concentration of gelator is decreased (Fig. S13, Supporting Information). As discussed elsewhere, the apparent p$K_a$ of a gelator is determined by its degree of aggregation and thus its concentration.[15, 40, 55] By analysis of the pH profiles and 2NapVG signal intensities, it is readily apparent that the assembly of the 2NapVG is strongly influenced by the presence of the 2NapFF. At 30% 2NapFF, the pH drop does not have a distinct increase at the apparent p$K_a$ of the 2NapVG (4.7 at 7 mg/mL 2NapVG). However, there is an inflection point at this pH value. The decrease in the signal intensity of the 2NapVG occurs significantly before the pH reaches the expected p$K_a$, although the rate of the decrease in signal increases after this pH. At 50% 2NapFF, the pH decrease has no obvious inflection points at the apparent p$K_a$ of

4.5. The intensity of the 2NapVG integral again decreases at a pH far higher than the apparent p$K_a$ of the 2NapVG. Only approximately 20% of the 2NapVG is detectable by NMR at its p$K_a$. At 70% 2NapFF, the pH data again shows no inflection. In the absence of 2NapFF, 2NapVG at 3 mg/mL concentration remains unassembled, even when the pH has fallen to 4.2 (Fig. S13, Supporting Information).

These data strongly suggest a co-assembly of the two gelators, at least at certain relative concentrations. At 50% and 30% 2NapFF, there is a fraction of the 2NapVG that seems to behave as expected in terms of the rate of signal decrease with pH. However, a significant fraction of the 2NapVG signal intensity decreases before the expected p$K_a$, implying that it is co-assembling with the 2NapFF.

Hence, we interpret the non-linear rheological data as being due to a spectrum of behaviour across the series of mixtures. The 2NapVG is exchanging in solution with aggregates determined by the 2NapFF in a "sergeants and soldiers" manner. Because of the fast exchange however, only a proportion of the 2NapVG is incorporated in the gel fibres formed by 2NapFF as the pH drops. The remainder of the 2NapVG will presumably be able to act as a surfactant as the gelling is occurring, potentially modifying the fibre network that is growing (again, we have previously shown that this type of LMWG can act as a surfactant[32, 35]). We stress here that this does not have to be a modification of the fibres themselves; rather it could be that the 2NapVG modifies the tendency of the 2NapFF fibres to entangle and cross-link. This would then affect the rheological data of the gel, without requiring a significant change in the morphology of the fibres. After the 2NapFF has gelled, the remainder of the 2NapVG will form fibres, contributing to the rheological data. Schematically, we illustrate this in Fig. 6. Hence, the gel's mechanical properties will be very sensitive to the absolute ratio of the 2NapFF and 2NapVG, as well as to

the kinetics of gelation, which will presumably determine how much 2NapVG is incorporated into the fibres that are being directed by the 2NapFF.

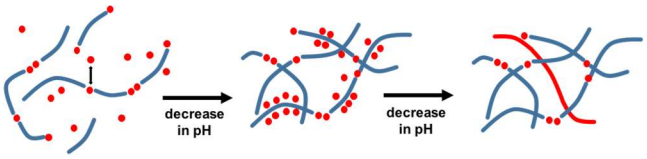


**Fig. 6.** Cartoon showing the assembly of a mixture of 2NapFF (blue) and 2NapVG (red). Partial co-assembly occurs as the pH drops, but the fast exchange of the 2NapVG from the micellar aggregates results in a fraction of the 2NapVG not being incorporated; this assembles alone as the pH drops further.

## Conclusions

Two component supramolecular gels are extremely complex. There is ever increasing interest in these multi-component systems, but there are few studies showing how the assembly is affected by the relative ratios of the components. It is clear from our data here that kinetics is an extremely important factor. For these pH-triggered gelators, there are non-linear effects in terms of the rheological data. Conceptually, the two components can inter-mix or remain independent at high pH, and then co-assemble or self-sort as the pH is decreased. Here, we have shown that the situation for a mixture of 2NapFF and 2NapVG is more complex than these simple either/or cases. At high pH, inter-mixing is occurring, at least to some degree. As the pH is decreased, there is a partial co-assembly of the two gelling components. From the NMR data, there are clearly two stages by which the 2NapVG assembles in the mixtures. The first stage is above the expected p$K_a$ of the 2NapVG. The fraction that assembles above this expected p$K_a$ depends on the mixture ratio. We assign this stage to co-assembly of both LMWG. At later times, the pH drops to the p$K_a$ of the 2NapVG and there is a different rate of assembly. Hence, we assign these

as a co-assembly stage and a stage where the 2NapVG assembles alone. When assembling alone, it is possible that the 2NapVG is forming an independent network, or it could be that it is assembling on the pre-formed mixed network. As a result of this complicated situation, the rheological data for the gels formed at different ratios of the two gelators are non-linear, despite the fibres forming the networks being similar in all cases.

We have shown previously for this family of gelator that self-sorting can be controlled by the differences in p$K_a$ for a number of examples.[27, 30-31] However, we have previously found one example where co-assembly occurred despite a difference in p$K_a$ of around one unit; this example involved two structurally similar gelators, which only differed by the terminal amino acid.[27] As such, it is clear that a difference in p$K_a$ is not a sufficient driving force for self-sorting. Whilst the current two gelators are not as structurally related as our co-assembling example, we also note that the system presented here involves one LMWG that forms persistent worm-like micelles. It may be that the type of micelle formed at high pH is important as our previous examples of effective self-sorting have been for systems where both gelators form non-persistent micelles at high pH. We note again that there are very limited data on mixed gelators and self-sorting or mixing and, in some cases, the type of assembly seems to be assumed as opposed to proven.[7] In this paper, we have shown that simple assumptions as to whether or not co-assembly or self-sorting are occurring in a system may not always hold and that simply mixing at one specific ratio is insufficient to truly understand these systems.

ASSOCIATED CONTENT

**Supporting Information**. Full experimental details, further rheological data, NMR data, SANS data and fits, SEM images, and pH titrations. The Supporting Information is available free of charge on the ACS Publications website.

AUTHOR INFORMATION

**Corresponding Author**

**Email:** dave.adams@glasgow.ac.uk

**Author Contributions**

The manuscript was written through contributions of all authors. All authors have given approval to the final version of the manuscript.

ACKNOWLEDGMENT

DA thanks the EPSRC for a Fellowship (EP/L021978/1), which also funded ED. The experiment at the Institut Laue Langevin was allocated beam time under experiment number 9-11-1802 (DOI: 10.5291/ILL-DATA.9-11-1802). This work benefitted from the SasView software, originally developed by the DANSE project under NSF award DMR-0520547. The NMR spectrometers used for this work were funded by the EPSRC (EP/K039687/1 and EP/C005643/1).

REFERENCES

1. Hirst, A. R.; Escuder, B.; Miravet, J. F.; Smith, D. K., High-Tech Applications of Self-Assembling Supramolecular Nanostructured Gel-Phase Materials: From Regenerative Medicine to Electronic Devices. *Angewandte Chemie International Edition* **2008,** *47* (42), 8002-8018.

2. Weiss, R. G., The Past, Present, and Future of Molecular Gels. What Is the Status of the Field, and Where Is It Going? *Journal of the American Chemical Society* **2014,** *136* (21), 7519-7530.
3. Skilling, K. J.; Citossi, F.; Bradshaw, T. D.; Ashford, M.; Kellam, B.; Marlow, M., Insights into low molecular mass organic gelators: a focus on drug delivery and tissue engineering applications. *Soft Matter* **2014,** *10* (2), 237-256.
4. Du, X.; Zhou, J.; Shi, J.; Xu, B., Supramolecular Hydrogelators and Hydrogels: From Soft Matter to Molecular Biomaterials. *Chemical Reviews* **2015,** *115* (24), 13165-13307.
5. Babu, S. S.; Praveen, V. K.; Ajayaghosh, A., Functional π-Gelators and Their Applications. *Chemical Reviews* **2014,** *114* (4), 1973-2129.
6. Buerkle, L. E.; Rowan, S. J., Supramolecular gels formed from multi-component low molecular weight species. *Chemical Society Reviews* **2012,** *41* (18), 6089-6102.
7. Raeburn, J.; Adams, D. J., Multicomponent low molecular weight gelators. *Chemical Communications* **2015,** *51* (25), 5170-5180.
8. Smith, M. M.; Smith, D. K., Self-sorting multi-gelator gels-mixing and ageing effects in thermally addressable supramolecular soft nanomaterials. *Soft Matter* **2011,** *7* (10), 4856-4860.
9. Moffat, J. R.; Smith, D. K., Controlled self-sorting in the assembly of 'multi-gelator' gels. *Chemical Communications* **2009,** (3), 316-318.
10. Alakpa, Enateri V.; Jayawarna, V.; Lampel, A.; Burgess, Karl V.; West, Christopher C.; Bakker, Sanne C. J.; Roy, S.; Javid, N.; Fleming, S.; Lamprou, Dimitris A.; Yang, J.; Miller, A.; Urquhart, Andrew J.; Frederix, Pim W. J. M.; Hunt, Neil T.; Péault, B.; Ulijn, Rein V.; Dalby, Matthew J., Tunable Supramolecular Hydrogels for Selection of Lineage-Guiding Metabolites in Stem Cell Cultures. *Chem 1* (2), 298-319.
11. Liyanage, W.; Nilsson, B. L., Substituent Effects on the Self-Assembly/Coassembly and Hydrogelation of Phenylalanine Derivatives. *Langmuir* **2016,** *32* (3), 787-799.
12. Felip-León, C.; Díaz-Oltra, S.; Galindo, F.; Miravet, J. F., Chameleonic, Light Harvesting Photonic Gels Based on Orthogonal Molecular Fibrillization. *Chemistry of Materials* **2016**.
13. Fichman, G.; Guterman, T.; Adler-Abramovich, L.; Gazit, E., Synergetic functional properties of two-component single amino acid-based hydrogels. *CrystEngComm* **2015,** *17* (42), 8105-8112.
14. Edwards, W.; Smith, D. K., Enantioselective Component Selection in Multicomponent Supramolecular Gels. *Journal of the American Chemical Society* **2014,** *136* (3), 1116-1124.
15. Tena-Solsona, M.; Escuder, B.; Miravet, J. F.; Casttelleto, V.; Hamley, I. W.; Dehsorkhi, A., Thermodynamic and Kinetic Study of the Fibrillization of a Family of Tetrapeptides and Its Application to Self-Sorting. What Takes So Long? *Chemistry of Materials* **2015,** *27* (9), 3358-3365.
16. Hsu, S.-M.; Wu, F.-Y.; Lai, T.-S.; Lin, Y.-C.; Lin, H.-C., Self-assembly and hydrogelation from multicomponent coassembly of pentafluorobenzyl-phenylalanine and pentafluorobenzyl-diphenylalanine. *RSC Advances* **2015,** *5* (29), 22943-22946.
17. Kölbel, M.; Menger, F. M., Molecular Recognition among Structurally Similar Components of a Self-Assembling Soft Material. *Langmuir* **2001,** *17* (15), 4490-4492.
18. Elsawy, M. A.; Smith, A. M.; Hodson, N.; Squires, A.; Miller, A. F.; Saiani, A., Modification of β-Sheet Forming Peptide Hydrophobic Face: Effect on Self-Assembly and Gelation. *Langmuir* **2016,** *32* (19), 4917-4923.

19. Ikeda, M.; Tanida, T.; Yoshii, T.; Kurotani, K.; Onogi, S.; Urayama, K.; Hamachi, I., Installing logic-gate responses to a variety of biological substances in supramolecular hydrogel–enzyme hybrids. *Nat Chem* **2014,** *6* (6), 511-518.
20. Onogi, S.; Shigemitsu, H.; Yoshii, T.; Tanida, T.; Ikeda, M.; Kubota, R.; Hamachi, I., In situ real-time imaging of self-sorted supramolecular nanofibres. *Nat Chem* **2016,** *8* (8), 743-752.
21. Görl, D.; Zhang, X.; Stepanenko, V.; Würthner, F., Supramolecular block copolymers by kinetically controlled co-self-assembly of planar and core-twisted perylene bisimides. *Nature Communications* **2015,** *6*, 7009.
22. Singh, N.; Zhang, K.; Angulo-Pachon, C. A.; Mendes, E.; van Esch, J. H.; Escuder, B., Tandem reactions in self-sorted catalytic molecular hydrogels. *Chemical Science* **2016,** *7* (8), 5568-5572.
23. Horgan, C. C.; Rodriguez, A. L.; Li, R.; Bruggeman, K. F.; Stupka, N.; Raynes, J. K.; Day, L.; White, J. W.; Williams, R. J.; Nisbet, D. R., Characterisation of minimalist co-assembled fluorenylmethyloxycarbonyl self-assembling peptide systems for presentation of multiple bioactive peptides. *Acta Biomaterialia* **2016,** *38*, 11-22.
24. Sandeep, A.; Praveen, V. K.; Kartha, K. K.; Karunakaran, V.; Ajayaghosh, A., Supercoiled fibres of self-sorted donor-acceptor stacks: a turn-off/turn-on platform for sensing volatile aromatic compounds. *Chemical Science* **2016,** *7* (7), 4460-4467.
25. Ardona, H. A. M.; Tovar, J. D., Energy transfer within responsive pi-conjugated coassembled peptide-based nanostructures in aqueous environments. *Chemical Science* **2015,** *6* (2), 1474-1484.
26. Li, D.; Shi, Y.; Wang, L., Mechanical Reinforcement of Molecular Hydrogel by Co-assembly of Short Peptide-based Gelators with Different Aromatic Capping Groups. *Chinese Journal of Chemistry* **2014,** *32* (2), 123-127.
27. Colquhoun, C.; Draper, E. R.; Eden, E. G. B.; Cattoz, B. N.; Morris, K. L.; Chen, L.; McDonald, T. O.; Terry, A. E.; Griffiths, P. C.; Serpell, L. C.; Adams, D. J., The effect of self-sorting and co-assembly on the mechanical properties of low molecular weight hydrogels. *Nanoscale* **2014,** *6* (22), 13719-13725.
28. Draper, E. R.; Lee, J. R.; Wallace, M.; Jackel, F.; Cowan, A. J.; Adams, D. J., Self-sorted photoconductive xerogels. *Chemical Science* **2016,** *7* (10), 6499-6505.
29. Raeburn, J.; Alston, B.; Kroeger, J.; McDonald, T. O.; Howse, J. R.; Cameron, P. J.; Adams, D. J., Electrochemically-triggered spatially and temporally resolved multi-component gels. *Materials Horizons* **2014,** *1* (2), 241-246.
30. Draper, E. R.; Eden, E. G. B.; McDonald, T. O.; Adams, D. J., Spatially resolved multicomponent gels. *Nat Chem* **2015,** *7* (10), 848-852.
31. Morris, K. L.; Chen, L.; Raeburn, J.; Sellick, O. R.; Cotanda, P.; Paul, A.; Griffiths, P. C.; King, S. M.; O'Reilly, R. K.; Serpell, L. C.; Adams, D. J., Chemically programmed self-sorting of gelator networks. *Nature Communications* **2013,** *4*, 1480.
32. Cardoso, A. Z.; Mears, L. L. E.; Cattoz, B. N.; Griffiths, P. C.; Schweins, R.; Adams, D. J., Linking micellar structures to hydrogelation for salt-triggered dipeptide gelators. *Soft Matter* **2016,** *12* (15), 3612-3621.
33. Chen, L.; McDonald, T. O.; Adams, D. J., Salt-induced hydrogels from functionalised-dipeptides. *RSC Advances* **2013,** *3* (23), 8714-8720.
34. Tang, C.; Smith, A. M.; Collins, R. F.; Ulijn, R. V.; Saiani, A., Fmoc-Diphenylalanine Self-Assembly Mechanism Induces Apparent pKa Shifts. *Langmuir* **2009,** *25* (16), 9447-9453.

35. Li, T.; Kalloudis, M.; Cardoso, A. Z.; Adams, D. J.; Clegg, P. S., Drop-Casting Hydrogels at a Liquid Interface: The Case of Hydrophobic Dipeptides. *Langmuir* **2014,** *30* (46), 13854-13860.
36. Chen, L.; Morris, K.; Laybourn, A.; Elias, D.; Hicks, M. R.; Rodger, A.; Serpell, L.; Adams, D. J., Self-Assembly Mechanism for a Naphthalene−Dipeptide Leading to Hydrogelation. *Langmuir* **2010,** *26* (7), 5232-5242.
37. Adams, D. J.; Butler, M. F.; Frith, W. J.; Kirkland, M.; Mullen, L.; Sanderson, P., A new method for maintaining homogeneity during liquid-hydrogel transitions using low molecular weight hydrogelators. *Soft Matter* **2009,** *5* (9), 1856-1862.
38. Draper, E. R.; Mears, L. L. E.; Castilla, A. M.; King, S. M.; McDonald, T. O.; Akhtar, R.; Adams, D. J., Using the hydrolysis of anhydrides to control gel properties and homogeneity in pH-triggered gelation. *RSC Advances* **2015,** *5* (115), 95369-95378.
39. Fleming, S.; Debnath, S.; Frederix, P. W. J. M.; Hunt, N. T.; Ulijn, R. V., Insights into the Coassembly of Hydrogelators and Surfactants Based on Aromatic Peptide Amphiphiles. *Biomacromolecules* **2014,** *15* (4), 1171-1184.
40. Chen, L.; Revel, S.; Morris, K.; C. Serpell, L.; Adams, D. J., Effect of Molecular Structure on the Properties of Naphthalene−Dipeptide Hydrogelators. *Langmuir* **2010,** *26* (16), 13466-13471.
41. Houton, K. A.; Morris, K. L.; Chen, L.; Schmidtmann, M.; Jones, J. T. A.; Serpell, L. C.; Lloyd, G. O.; Adams, D. J., On Crystal versus Fiber Formation in Dipeptide Hydrogelator Systems. *Langmuir* **2012,** *28* (25), 9797-9806.
42. Krężel, A.; Bal, W., A formula for correlating pKa values determined in D2O and H2O. *Journal of Inorganic Biochemistry* **2004,** *98* (1), 161-166.
43. Popov, K.; Ronkkomaki, H.; Lajunen, L. H. J., Guidelines for NMR Measurements for Determination of High and Low pKa Values. *Pure and Applied Chemistry* **2006,** *78* (3), 663-675.
44. Rodd, L. E.; Scott, T. P.; Cooper-White, J. J.; McKinley, G. H., Capillary Break-up Rheometry of Low-Viscosity Elastic Fluids. *Applied Rheology* **2005,** *15*, 12-27.
45. Campo-Deaño, L.; Clasen, C., The slow retraction method (SRM) for the determination of ultra-short relaxation times in capillary breakup extensional rheometry experiments. *Journal of Non-Newtonian Fluid Mechanics* **2010,** *165* (23–24), 1688-1699.
46. Langeveld-Voss, B. M. W.; Waterval, R. J. M.; Janssen, R. A. J.; Meijer, E. W., Principles of "Majority Rules" and "Sergeants and Soldiers" Applied to the Aggregation of Optically Active Polythiophenes: Evidence for a Multichain Phenomenon. *Macromolecules* **1999,** *32* (1), 227-230.
47. Foster, J. A.; Edkins, R. M.; Cameron, G. J.; Colgin, N.; Fucke, K.; Ridgeway, S.; Crawford, A. G.; Marder, T. B.; Beeby, A.; Cobb, S. L.; Steed, J. W., Blending Gelators to Tune Gel Structure and Probe Anion-Induced Disassembly. *Chemistry – A European Journal* **2014,** *20* (1), 279-291.
48. Nebot, V. J.; Escuder, B.; Miravet, J. F.; Smets, J.; Fernández-Prieto, S., Interplay of Molecular Hydrogelators and SDS Affords Responsive Soft Matter Systems with Tunable Properties. *Langmuir* **2013,** *29* (30), 9544-9550.
49. Reddy, A.; Sharma, A.; Srivastava, A., Optically Transparent Hydrogels from an Auxin–Amino-Acid Conjugate Super Hydrogelator and its Interactions with an Entrapped Dye. *Chemistry – A European Journal* **2012,** *18* (24), 7575-7581.

50. Orfi, L.; Lin, M.; Larive, C. K., Measurement of SDS Micelle−Peptide Association Using 1H NMR Chemical Shift Analysis and Pulsed-Field Gradient NMR Spectroscopy. *Analytical Chemistry* **1998,** *70* (7), 1339-1345.
51. Cornwell, D. J.; Daubney, O. J.; Smith, D. K., Photopatterned Multidomain Gels: Multi-Component Self-Assembled Hydrogels Based on Partially Self-Sorting 1,3:2,4-Dibenzylidene-d-sorbitol Derivatives. *Journal of the American Chemical Society* **2015,** *137* (49), 15486-15492.
52. Foster, J. S.; Żurek, J. M.; Almeida, N. M. S.; Hendriksen, W. E.; le Sage, V. A. A.; Lakshminarayanan, V.; Thompson, A. L.; Banerjee, R.; Eelkema, R.; Mulvana, H.; Paterson, M. J.; van Esch, J. H.; Lloyd, G. O., Gelation Landscape Engineering Using a Multi-Reaction Supramolecular Hydrogelator System. *Journal of the American Chemical Society* **2015,** *137* (45), 14236-14239.
53. Wallace, M.; Iggo, J. A.; Adams, D. J., *Submitted for Publication* **2016**.
54. Aufderhorst-Roberts, A.; Frith, W. J.; Kirkland, M.; Donald, A. M., Microrheology and Microstructure of Fmoc-Derivative Hydrogels. *Langmuir* **2014,** *30* (15), 4483-4492.
55. Wallace, M.; Iggo, J. A.; Adams, D. J., Using solution state NMR spectroscopy to probe NMR invisible gelators. *Soft Matter* **2015,** *11* (39), 7739-7747.